International Journal of Robotics and Control Systems
Vol. 4, No. 4, 2024, pp. 1561-1583
ISSN 2775-2658
http://pubs2.ascee.org/index.php/ijrcs

Fuzzy Control for Spacecraft Orbit Transfer with Gain Perturbations and Input Constraint

Sarah Nemmour [a,1,*], Bachir Daaou [a,2], Francis Okello [b,3]

[a] Automation School, Vision and Intelligent Systems Control Laboratory, USTO University, Oran, Algeria
[b] Mechanical Engineering School, Makerere University, Kampala, Uganda
[1] nemmours@gmail.com; [2] bachir.daaou@univ-usto.dz; [3] okellofrancis0@gmail.com
* Corresponding Author

ARTICLE INFO

Article history
Received August 02, 2024
Revised September 03, 2024
Accepted September 19, 2024

Keywords
Spacecraft Orbit Transfer;
Fuzzy T-S Model;
Lyapunov Theory;
Linear Matrix Inequality;
Convex Optimization;
Fuzzy Guaranteed Cost Control

ABSTRACT

This paper presents the problem of fuzzy guaranteed cost tracking control for spacecraft orbit transfer with parameter uncertainties and additive controller gain perturbations and subject to input constraints, and guaranteed cost function. The goal is to perform a planar orbit transfer in a circular orbit, focusing on minimizing fuel usage while accounting for uncertainties in both the plant and controller. Spacecraft dynamics is based on the Keplerian two-body problem using polar coordinates, which allows long-distance maneuvers in circular orbit when the well-known Clohessy-Wiltshire (C-W) equation is restricted by limited-distance maneuvers. To approximate the nonlinearities in the dynamical equation of motion, a Takagi-Sugeno (T-S) fuzzy model is proposed and a linearized model is established for the output tracking problem of the orbit transfer process. Issue related to the absence of a single equilibrium point in the nonlinear system, a gain-scheduling technique based on multiple operating points is employed to develop the (T-S) fuzzy model through the fuzzy approach. Based on the parallel distributed compensation (PDC) approach, sufficient conditions for a fuzzy non-fragile guaranteed cost control are derived. Using the Lyapunov theory, the controller objectives are formulated through linear matrix inequality (LMIs) which allows the system to be transferred into a convex optimization problem. The designed controller effectively accomplishes the orbit transfer process with minimal fuel consumption and maintains the performance level below a specified upper bound. Numerical simulations are conducted to demonstrate the effectiveness of the proposed method.

1. Introduction

Orbit transfer refers to the process of changing a spacecraft's initial orbit to reach a specific target orbit. After separation from the launch vehicle, a satellite is often placed close to, but not exactly on, its intended mission orbit. The spacecraft must change orbit one or more times to reach its precise mission orbit. Orbit transfer is often necessary for deployment, rendezvous with another spacecraft or asteroid, or to avoid potential threats.

In recent years, the spacecraft orbit transfer problem has rapidly gained interest. [1] used the Levi-Civita coordinates to solve the orbit transfer and rendezvous problems. [2] studied minimum-

fuel direct two-impulses orbit transfers from Gateway to Low Lunar Orbit. [3] addressed the automated orbital transfer and hovering control using feedback compensation. [4] investigated a trajectory optimization of low-thrust interplanetary and Earth orbital transfers. [5] discussed the minimum-time low-thrust transfer between Earth orbits using vectorial orbital elements. [6] studied the optimization of minimum-time low-thrust transfers using convex programming. These studies focus on the nonlinear dynamics of spacecraft, which can be addressed using various nonlinear control and optimization methods. In the context of linearized dynamics, relative motion is widely applied to orbit transfer and rendezvous problems. The dynamic model is represented by a set of linearized differential equations: if the target orbit is nearly circular, the (C-W) equations are used [7]. For an eccentric target orbit, the Tschauner-Hempel (T-H) equations are applied. Both models are restricted by the limited distance between the spacecraft's initial and final positions, making them inappropriate for long-distance maneuvers. The dynamics of spacecraft motion in this research are described using polar coordinates, where the motion is represented by a set of nonlinear differential equations. This model is mainly used for long-distance navigation and enables a clear understanding of radial and transverse velocity changes during orbit transfers.

On the other hand, the Takagi-Sugeno (T-S) fuzzy systems introduced by [8] are considered an effective way to model nonlinear systems using fuzzy logic. (T-S) fuzzy models can approximate any smooth nonlinear function with a high degree of accuracy, making them recognized as universal approximators [9], [10]. (T-S) systems are mainly based on fuzzy sets, fuzzy rules, and a collection of local linear models interconnected through fuzzy membership functions. The design procedure for the (T-S) model is achieved through the (PDC) concept [11], [12]. For each rule in the (T-S) fuzzy model, a linear feedback controller is specifically designed. This approach allows a more accurate approximation of nonlinear behaviors by combining local linear models, making it particularly useful in control systems and various other applications where managing uncertainty and nonlinearity is critical [13]-[17]. Furthermore, the gain-scheduling technique is a well-known technique for controlling certain classes of nonlinear systems and is commonly employed when a plant is subject to large changes in its operating state. The design method of gain scheduled controller involved selecting different operating points that reflect changes in system dynamics to cover the full range of the plant’s operating conditions. At each operating point, a linear time-invariant (LTI) controller is designed, and then the gains of the controller between these operating points are scheduled [18], [19]. In this research, the fuzzy technique based on the gain-scheduling approach is adopted to derive the linearized model of the equation of spacecraft motion described in polar coordinates. The strength of this model lies in its ability to accurately represent the original nonlinear system through high approximation using the fuzzy technique. Additionally, the gain-scheduling approach is well-suited for systems with significant state changes, making it effective for performing long-distance maneuvers. Another advantage is that the consequent part of a fuzzy rule operates as a linear dynamic subsystem, allowing the use of classical and well-developed linear control theory to address the spacecraft orbit transfer problem.

Many uncertain factors such as external disturbances in space, equipment malfunctions, and measurement errors can compromise both the precision and security of the orbital transfer process making it challenging to determine the spacecraft's accurate position and velocity. Furthermore, factors such as parameter drift, mass variation, and other factors affect the controller accuracy. The presence of these factors and their effects has inspired extensive research into orbital transfer control in the presence of uncertainties [20]-[23]. Furthermore, controller fragility can degrade the performance of the closed-loop system due to small variations in the controller design coefficients. Generally, avoiding perturbations during controller implementation is challenging due to factors such as inherent imprecision in analog systems, rapid changes in the operating point of a nonlinear system, the need for additional parameter tuning in the final controller setup, and other associated factors making it a critical aspect to address in practical controller design. Controllers designed can be very sensitive or fragile to errors in the controller coefficients, despite their robustness to plant uncertainties. In this research, the uncertainties are considered in both the controller gains and the

system dynamics. Significant efforts have been made to address the problem of designing uncertain non-fragile controllers [24]-[27]. However, the problem remains challenging.

Guaranteed cost control is an approach that offers a significant advantage in the control system. This method provides an upper bound on a given performance index, ensuring that the degradation of system performance due to model and controller uncertainties will not exceed this predetermined bound. By guaranteeing this upper limit, the approach enables more robust control designs that can better handle uncertainties while meeting specified performance criteria.

During a space mission, the capacity of the propellant equipment is another critical factor to consider, making it imperative to restrict energy usage during orbital maneuvers to conserve fuel and extend mission duration. The input constraint is an essential tool used to limit the fuel consumption of spacecraft during maneuvers. By imposing constraints on the control inputs, such as thrust levels, the control system can ensure that fuel usage is maintained within specified limits. This is particularly critical in space missions, where fuel is a limited and precious resource. Many research efforts have been carried out in this context to solve the minimum fuel orbit transfer problem using such constraints. [28], [29], studied a guaranteed cost control method for the homing phase of orbital rendezvous. The author utilized the (C-W) equations and accounted for uncertainties only within the system. [30] proposed a robust guaranteed cost controller to solve the orbit transfer problem with small thrust consumption. The author focused on low Earth rendezvous control, considering uncertainty solely in the system. In [31], the problem of non-fragile guaranteed cost control for low-Earth spacecraft orbit transfer with uncertainty and small thrust is investigated. In [32], the non-fragile H_∞ guaranteed cost control for spacecraft rendezvous is studied without considering the uncertainty in the system. [33] addressed the problem of non-fragile robust H_∞ control for spacecraft rendezvous with external perturbation. The research efforts that have been reported addressed the relative motion for the problem of rendezvous between the chaser and target, whether for low Earth orbit or the homing phase. The application of a linearized model for closed-loop linear control in long-distance spacecraft maneuvers is rarely addressed in the existing literature.

Based on the reported works, the existing results in the literature in terms of closed-loop linear control for the orbit transfer problem or spacecraft rendezvous are mainly using relative motion. Considerable attention has been devoted to investigating the relative motion control using the linearized dynamics where the (C-W) equation is mainly used for circular reference orbits. Here, it is well noticed that the precision of these linearized models decreases rapidly as the initial separation between initial and final positions increases. However, few results in the literature have presented the closed-loop linear control for long-distance orbital maneuvers, since the open-loop control methods are mainly intended for long-distance navigation processes. An another motivation for the present research was the control of orbit transfer using intelligent control, since this type of control is rarely used in orbital maneuver control problems.

Motivated by the previous discussions, this research addresses the problem of fuel minimum of orbit transfer maneuver with parameter uncertainties and controller gain perturbations. The dynamics of motion are described using the polar coordinates. To obtain a linearized model of the dynamic equation, the fuzzy theory approach is employed to approximate the nonlinearities in the equation of motion. The modeling is performed using the (T-S) paradigm by considering the gain-scheduling principle that relies on selecting several operating points in the system. The resulting model more approximately represents the original nonlinear system with approximation defined by the fuzzy membership function, this type of fuzzy model has not been implemented in the literature for the orbit transfer process. To perform an orbit transfer from a known initial position to a desired final position, we developed an output tracking system to ensure that the spacecraft tracks the desired target position in the final orbit. As an improvement, this research presents a fuzzy gain-scheduled (FGS) control to solve the problem of spacecraft orbit transfer with long-distance maneuvers. Given that designing a multi-objective controller for cases with uncertainties in both the system and the controller is challenging, this paper explores the development of a robust, and non-fragile fuzzy guaranteed cost state feedback controller. In addition to addressing uncertainties,

the designed controller focuses on minimizing fuel consumption by simultaneously considering the cost function and the input constraints. Based on Lyapunov theory, the sufficient conditions for a fuzzy, robust and non-fragile guaranteed cost controller are formulated using (LMI) framework. The closed-loop system is then converted into a stabilization problem, which is solved using a convex optimization method. Numerical simulations are presented, demonstrating two maneuver scenarios: from medium Earth orbit (MEO) to geostationary Earth orbit (GEO), and from low Earth orbit (LEO) to medium Earth orbit (MEO). Additionally, a comparison with an existing control method was carried out. These simulations confirmed the effectiveness of the proposed control design by achieving satisfactory tracking performance.

The manuscript is structured as follows: Section 2 introduces the fuzzy modeling of the spacecraft orbit transfer dynamics, covering a brief explanation of the dynamical system modeling, selection of state variables, altitude, and velocity range, and a detailed discussion of the various control objectives. Section 3 describes the design of a fuzzy non-fragile guaranteed cost control strategy for the orbit transfer process, using the (PDC) scheme. In Section 4, a numerical example is provided to demonstrate the effectiveness of the proposed control method. Finally, Section 5 concludes the manuscript.

2. Problem Formulation

A planar orbit transfer between two circular orbits is addressed in this manuscript, with the dynamic equation of motion described by polar coordinates. Utilizing the fuzzy approach, a (T-S) model is developed to represent the nonlinear dynamics of spacecraft motion. This model is characterized by fuzzy IF-THEN rules. Our objective is to design a controller for the orbit transfer problem from a given initial position to the desired position located in the final orbit. In accordance with the study's objectives, the spacecraft is considered to be a point-mass object, with a state vector completely determined by its position and velocity vectors (r, υ) as shown in Fig. 1.

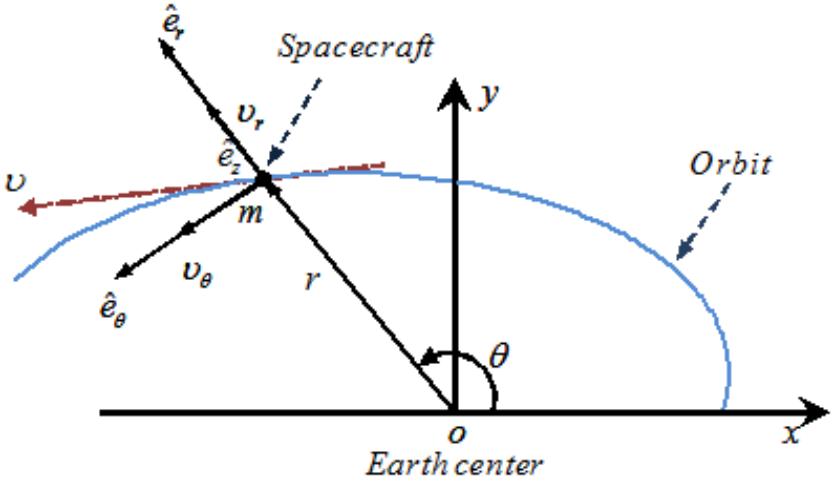

Fig. 1. Spacecraft trajectory for the orbit transfer mission

The earth center is located at the origin of the xy-frame. The spacecraft's center of mass is at the origin of the $(\hat{e}_r, \hat{e}_\theta, \hat{e}_z)$ basis vector. The motion of the spacecraft is described by the following set of differential equations, considering the Keplerian two-body dynamic model [34].

$$\dot{x} = f(x,u,t) = \begin{cases} \dot{r} = \upsilon \\ \dot{\upsilon} = G(r) + u \end{cases}$$

Where, u is the control vector of the spacecraft, and $G(r)$ is the gravitational acceleration vector. The position vector $r$with respect to an inertial frame is expressed in polar coordinates $r$and θ, and the velocity vector υ is expressed in the radial-transversal reference frame by means of the radial $\upsilon_r$and transverse $\upsilon_\theta$components respectively. Assuming the spacecraft orbit is circular and the dynamical equations of spacecraft motion are given by [6].

$$\begin{cases} \dot{r} = v_r \\ \dot{\theta} = \dfrac{v_\theta}{r} \\ \dot{v}_r = -\dfrac{\mu}{r^2} + \dfrac{v_\theta^2}{r} + u_r \\ \dot{v}_\theta = -\dfrac{v_r v_\theta}{r} + u_\theta \end{cases} \quad (1)$$

This equation describes the trajectory of a spacecraft in its orbit. The trajectory of spacecraft can be understood by examining how its position, velocity, and acceleration change over time. $u_r$denotes the component of control thrust in the radial direction, u_θ denotes the control component in the transversal direction, and$\mu$is the Earth's gravitational parameter.

2.1. T-S Fuzzy Modeling of Equation of Motion

According to (1), we define the state vector$X(t) = [r(t), \theta(t), v_r(t), v_\theta(t)]^T$, the control input vector $U(t) = [U_r(t), U_\theta(t)]^T$, where, U_r and U_θ are the control thrust along the redial and the transversal directions respectively, and the output vector $Y(t) = [r(t), \theta(t)]^T$. A state-space representation for equation (1) can be expressed as follows.

$$\begin{bmatrix} \dot{X}(t) \\ Y(t) \end{bmatrix} = \begin{bmatrix} A & B \\ C & 0 \end{bmatrix} \begin{bmatrix} X(t) \\ U(t) \end{bmatrix} \quad (2)$$

$$A = \begin{bmatrix} 0 & 0 & 1 & 0 \\ 0 & 0 & 0 & \frac{1}{r} \\ -\frac{\mu}{r^3} & 0 & 0 & \frac{v_\theta}{r} \\ 0 & 0 & \frac{-v_\theta}{r} & 0 \end{bmatrix}, B = \begin{bmatrix} 0 & 0 \\ 0 & 0 \\ 1 & 0 \\ 0 & 1 \end{bmatrix}, C = \begin{bmatrix} 1 & 0 \\ 0 & 1 \\ 0 & 0 \\ 0 & 0 \end{bmatrix}^T.$$

Our objective is to develop a (T-S) fuzzy model for equation (2), The methodology proposed in [35] is adopted for this paper. First, we select p operating points for the nonlinear system and create a (LTI) model for each of these operating points. Let $z_l(l = 1, \ldots, g)$ be a premise variable that recognizes the operating points. We will use z (t) to define the vector containing elements$z_1(t) \cdots z_g(t)$. Let$M_{li}(i = 1, \ldots, s)$ be fuzzy sets of$z_l$and s is the number of model rules. The fuzzy model of the plant for the ith operating point is represented by the subsequent fuzzy rules. Rule i. If $z_1 = M_{1i}$ and … and$z_g = M_{gi}$, then the plant system is described by.

$$\begin{cases} \dot{X}(t) = A_i X(t) + BU(t) \\ Y(t) = CX(t) \quad \text{(i=1,...,s)} \end{cases} \quad (3)$$

The pairs(A_i, B, C) of the equation (3) are stabilizable and detectable. The matrix B is constant, A changes depending on the values of the radius r and the velocityv_θ, the radius $r(t)$ and the transverse velocity $v_\theta(t)$ are selected as the premise variables. Implementing the above-mentioned approach to the equation of motion for the spacecraft, two levels and two values are assigned to each premise variable. These consist of low altitude ('low (r_l)') and high altitude ('high (r_h)') for the radius, along with small value ('small (v_{θ_s})') and big value ('big (v_{θ_b})') for the transversal velocity. The nonlinear model outlined in equation (1) can then be represented using a (T-S) fuzzy model incorporating $4(2)^2$ fuzzy rules. The ranges are specified as $r_l \le r \le r_h$ and $v_{\theta_l} \le v_\theta \le v_{\theta_h}$ respectively. To cover all operating points, fuzzy rules were established for the following four operating points: $(r, v_\theta) = (r_l, v_{\theta_s}), (r_l, v_{\theta_b}), (r_h, v_{\theta_s}), (r_h, v_{\theta_b})$, and a (LTI) model was constructed for each operating point. The operating points are selected based on two key criteria. The first is identifying specific points where significant changes in the system dynamics occur. The second is ensuring that these points encompass all critical operational regions, ranging

from very low Earth altitude and small spacecraft velocity to very high Earth altitude and big spacecraft velocity, covering a wide transfer range.

Then, the T-S fuzzy model for the nonlinear system described in equation (2) is formulated through the subsequent four-rule fuzzy model.

- Rule 1. If r is low (r_l) and v_θ is small(v_{θ_s}), then

$$\begin{cases}\dot{X}(t) = A_1X(t) + BU(t)\\ Y(t) = CX(t)\end{cases}$$

- Rule 2. If r is low (r_l) and v_θ is big(v_{θ_b}), then

$$\begin{cases}\dot{X}(t) = A_2X(t) + BU(t)\\ Y(t) = CX(t)\end{cases}$$

- Rule 3. If r is high (r_h) and v_θ is small(v_{θ_s}), then

$$\begin{cases}\dot{X}(t) = A_3X(t) + BU(t)\\ Y(t) = CX(t)\end{cases}$$

- Rule 4. If r is high (r_h) and v_θ is big(v_{θ_b}), then

$$\begin{cases}\dot{X}(t) = A_4X(t) + BU(t)\\ Y(t) = CX(t)\end{cases}$$

$\omega_r(r)$ and $\omega_{v_\theta}(v_\theta)$ represent the membership functions that characterize r and v_θ respectively. These membership functions for rules 1-4 are defined as follows

$$\begin{cases}\omega_r(r_l) = \dfrac{r(t) - min_{r(t)}}{max_{r(t)} - min_{r(t)}}\\ \omega_r(r_h) = 1 - \omega_r(r_l)\end{cases}$$
$$\begin{cases}\omega_{v_\theta}(v_{\theta_s}) = \dfrac{v_\theta(t) - min_{v_\theta(t)}}{max_{v_\theta(t)} - min_{v_{\theta(t)}}}\\ \omega_{v_\theta}(v_{\theta_b}) = 1 - \omega_{v_\theta}(v_{\theta_s})\end{cases}$$

where, r_l and r_h represent 'low (l)' and 'high (h)' of r, respectively. However, v_{θ_s} and $v_{\theta b}$ represent 'small (s)' and 'big (b)' of v_θ, respectively. Then, we introduce h_i as follows.

$$h_i(z(t)) = \omega_r(r) \wedge \omega_{v_\theta}(v_\theta) \tag{4}$$

Where $(i = 1, \ldots, 4)$. Given that $\wedge$ represents the minimum operator in fuzzy logic, it follows.

$$h_1(z(t)) = \omega_r(r_l) \wedge \omega_{v_\theta}(v_{\theta_s})$$
$$h_2(z(t)) = \omega_r(r_l) \wedge \omega_{v_\theta}(v_{\theta_b})$$
$$h_3(z(t)) = \omega_r(r_h) \wedge \omega_{v_\theta}(v_{\theta_s})$$
$$h_4(z(t)) = \omega_r(r_h) \wedge \omega_{v_\theta}(v_{\theta_b})$$

And the fuzzy membership functionsω_r, ω_{v_θ} of r and v_θ are illustrated in the following Fig. 2.

Thus, the T-S fuzzy model which represents the nonlinear equation of spacecraft motion (1) is obtained as.

$$\begin{cases}\dot{X}(t) = \sum_{i=1}^{4} h_i(z(t))[A_iX(t) + BU(t)]\\ Y(t) = CX(t)\end{cases} \tag{5}$$

Moreover, defining α_i as

$$\alpha_i(z(t)) \triangleq \frac{h_i(z(t))}{\sum_{i=1}^{4} h_i(z(t))} \tag{6}$$

Where

$$\alpha_i(z(t)) \geq 0, \sum_{i=1}^{4} \alpha_i(z(t)) = 1$$

Then, a polytopic fuzzy model is obtained that corresponds to the entire operating range, thus, the system can be described by.

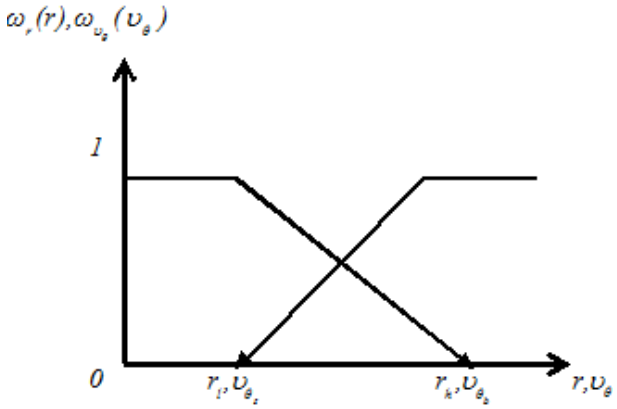

Fig. 2. Membership functions of r andυ_θ

$$\begin{cases} \dot{X}(t) = \sum_{i=1}^{4} \alpha_i(z(t)) \{A_i X(t) + BU(t)\} \\ Y(t) = CX(t) \end{cases} \tag{7}$$

2.2. Uncertainty Parameters

Due to external perturbation forces existing in space and the detection errors of equipment, it becomes particularly difficult to accurately determine the velocity and position of the spacecraft. This difficulty can affect the accuracy of the control force. Additionally, there also exist some inevitable factors such as thrust errors due to incomplete fuel burning and potential parameter drift during spacecraft maneuvers. Considering these unmodeled uncertainties, the resulting system can be given by.

$$\begin{cases} \dot{X}(t) = \sum_{i=1}^{4} \alpha_i\,(z(t))\left[\tilde{A}_i X(t) + BU(t)\right] \\ Y(t) = CX(t), \quad i = 1,\ldots,4. \end{cases} \tag{8}$$

Where

$$\tilde{A}_i = A_i + \Delta A_i$$

ΔA_i denote unknown time-varying matrices which are assumed to be norm bounded and tacking the form.

$$\Delta A_i = \Phi_i \Lambda_i(t) \Gamma_i$$

WhereΦ_i, Γ_i are known constant matrices with suitable dimensions and $\Lambda_i(t)$ denote unknown time-varying matrices with Lebesgue measurable elements restricted by.

$$\Lambda_i^T(t)\Lambda_i(t) \leq I$$

2.3. Output Tracking

Defining a reference output$Y_{tr}(t) = (r_{tr}(t), \theta_{tr}(t))$, the objective is to design a fuzzy output tracking controller such that the system output $Y(t)$ can asymptotically track the reference position$Y_{tr}(t)$. Let us define the output tracking error as.

$$\lim_{t\to\infty}(Y(t) - Y_{tr}(t)) = 0$$

We aim to eliminate the positional tracking error by introducing an integral action as follows.

$$Z(t) = \int_0^{t_f}(Y(\tau) - Y_{tr}(\tau))d\tau$$

Therefore

$$\dot{Z}(t) = Y(t) - Y_{tr}(t)$$

The resulting augmented system is formulated in the following form.

$$\begin{cases}\dot{W}(t) = \sum_{i=1}^{4}\alpha_i(t)\{(\bar{A}_i + \Delta\bar{A}_i)W(t) + \bar{B}U(t)\} + DY_{tr}(t)\\ Y(t) = \bar{C}W(t)\end{cases} \quad (9)$$

Where

$$\Delta\bar{A}_i = \bar{\Phi}_i\bar{\Lambda}_i(t)\bar{\Gamma}_i$$

The augmented matrices in system (9) are given as below

$$\bar{A}_i = \begin{bmatrix}A_i & 0\\ C & 0\end{bmatrix},\ \bar{B} = \begin{bmatrix}B\\ 0\end{bmatrix},\ \bar{C} = [C \quad 0],\ D = \begin{bmatrix}0\\ -I\end{bmatrix},\ W(t) = \begin{bmatrix}X(t)\\ Z(t)\end{bmatrix},$$

Furthermore, the augmented form of the uncertainty matrices are given as follows

$$\bar{\Phi}_i = \begin{bmatrix}\Phi_i & 0\\ 0 & 0\end{bmatrix},\ \bar{\Gamma}_i = \begin{bmatrix}\Gamma_i & 0\\ 0 & 0\end{bmatrix}, \bar{\Lambda}_i(t) = \begin{bmatrix}\Lambda_i(t) & 0\\ 0 & 0\end{bmatrix}.$$

Consequently, we have

$$\bar{\Lambda}_i^T(t)\bar{\Lambda}_i(t) \leq I$$

Therefore, the equation (9) is formulated as follows

$$\begin{cases}\dot{W}(t) = \sum_{i=1}^{4}\alpha_i(t)\left\{(\bar{\bar{A}}_i)W(t) + \bar{B}U(t)\right\} + DY_{tr}(t)\\ Y(t) = \bar{C}W(t)\end{cases} \quad (10)$$

Where

$$\bar{\bar{A}}_i = \bar{A}_i + \Delta\bar{A}_i$$

The fuzzy state feedback controller for the uncertain system (10) is deduced using the (PDC) stability concept as

$$U(t) = \sum_{i=1}^{4}\alpha_i(t)\,[K_{ix}X(t) + K_{iz}Z(t)]$$

Where, $K_i = [K_{ix} \quad K_{iz}]$ and $i = (1,\ldots,4)$. The fuzzy controller can be written as follows.

$$U(t) = \sum_{i=1}^{4} \alpha_i(t)\, K_i W(t) \tag{11}$$

Considering the gain perturbations, the non-fragile controller is formulated as follows

$$U(t) = \sum_{i=1}^{4} \alpha_i(t)\, [(K_i + \Delta K_i) W(t)] \tag{12}$$

Where K_i denote the nominal gains and ΔK_i denote the gain perturbations which have the following form.

$$\Delta K_i = \Theta_i \Delta_i(t) \Pi_i$$

Where, $\Theta_i$and Π_i are known constant matrices and $\Delta_i(t)$ denotes unknown time-varying matrices bounded by.

$$\Delta_i^T(t)\Delta_i(t) \leq I$$

Therefore, the resulting closed-loop system can be described as follows.

$$\begin{cases} \dot{W}(t) = \sum_{i=1}^{4} \alpha_i(t)\{(\bar{A}_i + \Delta\bar{A}_i) + \bar{B}(K_j + \Delta K_j) W(t)\} + DY_{tr}(t) \\ Y(t) = \bar{C} W(t) \end{cases} \tag{13}$$

2.4. Performance Cost and Energy Constraint

Considering the limited capacity of the propellant storage, it is essential to impose constraints on the control input within specific limits. For this end, we address the input constraints for the orbit transfer process in both the radial and transverse directions as follows.

$$\begin{cases} -\bar{U}_r \leq U_r \leq \bar{U}_r \\ -\bar{U}_\theta \leq U_\theta \leq \bar{U}_\theta \end{cases} \tag{14}$$

Where, U_r and U_θ define the rth and the θth element in the control input$U$. $\bar{U}_r$ and $\bar{U}_\theta$ represent the upper limits on thrust generated by the spacecraft propellants along each axial direction.

On the other hand, the quadratic cost is another significant requirement which is adopted in this paper. Q is the state weighting matrix and R is the control weighting matrix, by specifying the $R \succ 0$ and$Q \succ 0$, and considering the control law in (12), the performance level can be concisely formulated as.

$$J_{ot} = \int_0^{t_f} [U^T(\tau) R U(\tau) + W^T(\tau)\, Q W(\tau)] d\tau \tag{15}$$

Then, a fuzzy non-fragile guaranteed cost control law in the form (12) is synthesized such that the closed-loop system (13) achieves asymptotic stability and the performance level of the orbit transfer J_{ot} is less than or equals an upper bound $\bar{J}_{ot}$.

3. Controller Design

A fuzzy gain-scheduled guaranteed cost controller is designed to solve the orbit transfer problem. The designed controller has to ensure the global stability of the closed-loop system over the selected operating range. In this research, the input constraint and the cost function are considered in addition to the uncertainties of the model and controller. Firstly, a fuzzy non-fragile

guaranteed cost controller (FNGCC) is designed to make the spacecraft track the reference position located in the final orbit. Then, an optimal fuzzy non-fragile guaranteed cost controller (OFNGCC) is designed to solve the orbit transfer with a bounded thrust and minimum performance level. The following Lemmas are recalled to be utilized in our later development.

- Lemma 1 [36] Given real matrices L, E and S of suitable dimension with $S^TS \leq I$, then, for any positive scalar $\eta \succ 0$,

$$L^TSE + E^TS^TL \leq \eta L^TL + \eta^{-1}E^TE$$

- Lemma 2 [37] (Schur complement Lemma) Let Zbe a given symmetric matrix, the following statements are equivalents

1. 1.$Z \triangleq \begin{bmatrix} Z_{11} & Z_{12} \\ Z_{12}^T & Z_{22} \end{bmatrix} \succ 0$
2. $Z_{11} \succ 0, \quad Z_{22} - Z_{12}^T Z_{11}^{-1} Z_{12}$
3. 3.$Z_{22} \succ 0, \quad Z_{22} - Z_{12} Z_{22}^{-1} Z_{12}^T$

- Lemma 3 Given real matrices$F$, $G$of suitable dimensions, for any positive scalar ε the following inequality is satisfied

$$\begin{bmatrix} 0 & GF^T \\ FG^T & 0 \end{bmatrix} \leq \begin{bmatrix} \varepsilon GG^T & 0 \\ 0 & \varepsilon^{-1}FF^T \end{bmatrix}$$

- Lemma 4 [38] The parameterized linear matrix inequalities

$$\sum_{i=1}^{k}\sum_{j=1}^{k} \alpha_i\alpha_j \Upsilon_{ij} \prec 0$$

Is fulfilled, if the following conditions are satisfied

$$\Upsilon_{ii} \prec 0$$

$$\frac{1}{k-1}D_{ii} + \frac{1}{2}(D_{ij} + D_{ji}) \prec 0, \quad 1 \leq i \neq j \leq k$$

Proposition 1 For the fuzzy uncertain system (13), if there exist a symmetric positive definite matrix$P$, matricesK_j, $(j = 1,\ldots,4)$ and a positive scalar λ such that, the following matrix inequality holds for all permissible uncertainties $\sum_{i=1}^{4}\sum_{j=1}^{4} \alpha_i(t)\alpha_j(t)$.

$$\left[P\tilde{\tilde{A}}_i + \tilde{\tilde{A}}_i^T P + P\bar{B}(K_j + \Delta K_j) + (K_j + \Delta K_j)^T\bar{B}^TP + \lambda^{-1}PDD^TP + Q + (K_j + \Delta K_j)^TR(K_j + \Delta K_j)\right] \prec 0 \qquad (16)$$

Hence, the fuzzy control law $U(t) = \sum_{i=1}^{4} \alpha_i(t)\,(K_i + \Delta K_i)W(t)$ is robust fuzzy non-fragile guaranteed cost controller of the closed-loop system (13), and the quadratic performance level (15) has an upper bound of.

$$\bar{J}_{ot} = W^T(0)PW(0) + \lambda\int_0^t Y_{tr}^T(\tau)\,Y_{tr}(\tau)d\tau \qquad (17)$$

Proof: Defining a Lyapunov function

$$V(t) = W^T(t)PW(t)$$

Taking the time derivative of $V(t)$, one has

$$\dot{V}(t) = \dot{W}^T(t)PW(t) + W^T(t)P\dot{W}(t) = \sum_{i=1}^{4}\sum_{j=1}^{4}\left\{\left(W^T(t)\left(\tilde{\tilde{A}}_i + \bar{B}(K_j + \Delta K_j)\right)^T + Y_{tr}^T(t)D^T\right)PW(t) + W^T(t)P\left(\left(\tilde{\tilde{A}}_i + \bar{B}(K_j + \Delta K_j)\right)W(t) + DY_{tr}(t)\right)\right\}$$

Applying Lemma 1, one obtains

$$Y_{tr}^T(t)D^TPW(t) + W^T(t)PDY_{tr}(t) \leq \lambda^{-1}W^T(t)PDD^TPW(t) + \lambda Y_{tr}^T(t)Y_{tr}(t)$$

Therefore

$$\dot{V}(t) \leq \sum_{i=1}^{4}\sum_{j=1}^{4} \alpha_i \alpha_j \left[W^T(t)\left(\left(\tilde{\bar{A}}_i + \bar{B}(K_j + \Delta K_j)\right)^T P + P\left(\tilde{\bar{A}}_i + \bar{B}(K_j + \Delta K_j)\right) + \lambda^{-1} PDD^T P\right) W(t) + \lambda Y_{tr}^T(t) Y_{tr}(t)\right]$$

From the inequality (16), the latter inequality can be changed as follows

$$\begin{aligned} \dot{V}(t) \quad &\leq W^T(t)\{-Q - (K_j + \Delta K_j)^T R(K_j + \Delta K_j)\} W(t) + \lambda Y_{tr}^T(t) Y_{tr}(t) \\ &\leq -\{W^T(t) Q W(t) + U^T(t) R U(t)\} + \lambda Y_{tr}^T(t) Y_{tr}(t) \end{aligned} \tag{18}$$

For $Q = Q^T \geq 0$, $R = R^T \geq 0$ and $\lambda \succ 0$, we have

$$\dot{V}(t) \leq 0$$

From Lyapunov theory, the closed-loop fuzzy uncertain system in (13) is asymptotically stable. Integrating both sides of (18) from 0 to t_f, one obtains

$$\int_0^{t_f} \{W^T(t) Q W(t) + U^T(t) R U(t)\}\ dt \leq W^T(0) P W(0) + \lambda \int_0^{t_f} Y_{tr}^T(t) Y_{tr}(t)\ dt$$

Therefore, the performance level $\bar{J}_{ot}$ in (17) can be obviously obtained.

Proposition 2 [39] Consider the fuzzy system described in (13) with the fuzzy controller given by (12). The control thrust $U(t)$ is enforced into a definite region under the following constraints

$$-\bar{U}_\kappa \leq U_\kappa \leq \bar{U}_\kappa, \quad \kappa = (r, \theta)$$

If there exist $\beta \succ 0$, matrices K_j, and positive symmetric matrices P and H_i such that the matrix inequality (16) holds for.

$$W(0) P W^T(0) \leq \beta \tag{19}$$

$$\begin{bmatrix} H_i & (K_j + \Delta K_j) \\ (K_j + \Delta K_j)^T & \beta^{-1} P \end{bmatrix} \geq 0, \quad (i = 1, \ldots, 4) \tag{20}$$

$$(H_i)_{\kappa\kappa} \leq \bar{U}_\kappa^2, \quad \kappa = (r, \theta) \tag{21}$$

Then, $U(t) = \sum_{i=1}^{4} \alpha_i(t)\,[(K_i + \Delta K_i) W(t)]$ is a fuzzy non-fragile guaranteed cost controller which fulfils the input constraint (14) of the controlled system (13).

Proof: According to Proposition1, $U(t)$ is a fuzzy non-fragile guaranteed cost controller of the system (13), and P is a Lyapunov matrix by which the stability of the closed-loop system is fulfilled. Hence, the state trajectory of the closed-loop system satisfies

$$W^T(t) P W(t) \leq W^T(0) P W(0) \leq \beta$$

By Schur Complement, the matrix inequality (20) is equivalent to

$$\beta (K_j + \Delta K_j)^T P^{-1} (K_j + \Delta K_j) \leq H_i.$$

Let us define the κth component of each matrix K_j by $K_{j\kappa}$, one has

$$\begin{aligned} \left\| U_{j\kappa}(t) \right\|_2^2 &= U_{j\kappa}^T(t) U_{j\kappa}(t) = (K_{j\kappa} + \Delta K_{j\kappa})^T W^T(t) (K_{j\kappa} + \Delta K_{j\kappa}) W(t) \\ &= (K_{j\kappa} + \Delta K_{j\kappa})^T P^{-1} (K_{j\kappa} + \Delta K_{j\kappa}) W^T(t) P W(t) \\ &\leq (K_{j\kappa} + \Delta K_{j\kappa})^T P^{-1} (K_{j\kappa} + \Delta K_{j\kappa}) \beta \leq (H_i)_{\kappa\kappa} \end{aligned}$$

Where $(i = 1, \ldots, 4)$, $(j = 1, \ldots, 4)$, and $(\kappa = r, \theta)$.

From the inequality (21), it is obvious that the control law satisfies the input constraint (14).

Our next objective is to convert the obtained conditions in Proposition 1 and Proposition 2 to (LMIs). The following theorem is built on the basis of Lemma 4 and uses the aforementioned results to solve the robust fuzzy guaranteed cost tracking controller for the orbit transfer problem through convex optimization.

Theorem 1 Considering the uncertain orbit transfer system in (13) and the control law in (12), under the input constraint (14), the closed-loop system is asymptotically stable with an upper bound on the performance level, bounded thrust if there exist positive scalars β,λ,γ_ι where$(\iota = 1,\ldots,3)$, matrices $Y_j$and positive symmetric matrices X and H_i with proper dimensions satisfying the following matrix inequalities.

$$\Upsilon_{ii} \prec 0, (i = 1,\ldots,4) \tag{22}$$

$$\frac{1}{k-1}\Upsilon_{ii} + \frac{1}{2}\left(\Upsilon_{ij} + \Upsilon_{ji}\right) \prec 0, (1 \le i \ne j \le 4) \tag{23}$$

$$\begin{bmatrix} 1 & W^T(0) \\ W(0) & X \end{bmatrix} \ge 0 \tag{24}$$

$$\begin{bmatrix} H_i + \gamma_3\Theta_j\Theta_j^T & Y_j & \Pi_j X \\ * & X & 0 \\ * & * & \gamma_3 I \end{bmatrix} \ge 0, (j = 1,\ldots,4) \tag{25}$$

$$(H_i)_{\kappa\kappa} + \gamma_3 diag\{\Theta_j\Theta_j^T\} \le \bar{U}_\kappa^2, \kappa = (r,\theta) \tag{26}$$

Where

$$\Upsilon_{ij} = \sum_{i=1}^{4}\sum_{j=1}^{4}\alpha_i(t)\alpha_j(t) \begin{bmatrix} \Psi & \Omega_{12}^T & X & \Omega_{14} \\ * & \Omega_{22} & 0 & 0 \\ * & * & -\beta Q^{-1} & 0 \\ * & * & * & \Omega_{44} \end{bmatrix} \tag{27}$$

And

$$\Psi = sym\{\bar{A}_i X + \bar{B}Y_j\} + \gamma_1\bar{\Phi}_i\bar{\Phi}_i^T + \gamma_2\bar{B}\Theta_j\Theta_j^T\bar{B}^T$$

$$\Omega_{12} = Y_j + \gamma_2\Theta_j\Theta_j^T\bar{B}^T$$

$$\Omega_{22} = -\beta R^{-1} + \gamma_2\Theta_j\Theta_j^T$$

$$\Omega_{14} = \{\sqrt{\beta}D \quad \bar{\Gamma}_i X \quad \Pi_j X\}$$

$$\Omega_{44} = \{-\lambda I \quad -\gamma_1 I \quad -\gamma_2 I\}$$

Then, the desired state-feedback controller is expressed by$U(t) = \sum_{j=1}^{4}\alpha_j(t)\,Y_j X^{-1} W(t)$.

Proof: Considering the matrix inequalities (20) in the proposition 2, by doing a pre- and post-multiplication by matrix$diag\{I, \beta P^{-1}\}$, the latter matrix inequality is equivalent to.

$$\begin{bmatrix} H_i & (K_j + \Delta K_j)\beta P^{-1} \\ * & \beta P^{-1} \end{bmatrix} \ge 0 \tag{28}$$

Defining $X = \beta P^{-1}$ and $Y_j = K_j X$ where$(j = 1,\ldots,4)$, the matrix inequality (28) is obviously equivalent to.

$$\begin{bmatrix} H_i & Y_j + \Theta_j\Delta_j\Pi_j X \\ * & X \end{bmatrix} \ge 0 \tag{29}$$

Applying Lemma 1 and Lemma 3, inequality (29) can be written as

$$\begin{bmatrix} H_i + \gamma_3 \Theta_j \Theta_j^T & Y_j \\ * & X + \gamma_3^{-1} X \Pi_j^T \Pi_j X \end{bmatrix} \geq 0$$

Applying Lemma 2, LMI (25) is obviously obtained.

$$\begin{bmatrix} H_i + \gamma_3 \Theta_j \Theta_j^T & Y_j \\ * & X + \gamma_3^{-1} X \Pi_j^T \Pi_j X \end{bmatrix} \geq 0$$

Furthermore, by using schur complement and taking $X = \beta P^{-1}$, it follows that the inequality in (19) is equivalent to the inequality in (24).

From Proposition 1, performing a Pre- and post-multiplication of $\beta^{1/2} P^{-1}$ by the left-hand side of the inequality (16), one obtains

$$\sum_{i=1}^{4}\sum_{j=1}^{4} \alpha_i \alpha_j \Big\{ \beta \big[(\bar{A}_i + \bar{\Phi}_i \bar{\Lambda}_i \bar{\Gamma}_i) + \bar{B}(K_j + \Theta_j \Delta_j \Pi_j) \big] P^{-1} + \beta P^{-1} \big[(\bar{A}_i + \bar{\Phi}_i \bar{\Lambda}_i \bar{\Gamma}_i) + \bar{B}(K_j + \Theta_j \Delta_j \Pi_j) \big]^T + \beta P^{-1} Q P^{-1} + \beta \lambda^{-1} D D^T + \beta P^{-1} (K_j + \Theta_j \Delta_j \Pi_j)^T R (K_j + \Theta_j \Delta_j \Pi_j) P^{-1} \Big\} \prec 0$$

The latter inequality can be further expressed as.

$$\sum_{i=1}^{4}\sum_{j=1}^{4} \alpha_i \alpha_j \Big\{ \bar{A}_i X + X \bar{A}_i^T + \bar{B} Y_j + Y_j^T \bar{B} + \beta X Q X + \beta \lambda^{-1} D D^T + \big[(\bar{\Phi}_i \bar{\Lambda}_i \bar{\Gamma}_i) + \bar{B}(\Theta_j \Delta_j \Pi_j) \big] X + X \big[(\bar{\Phi}_i \bar{\Lambda}_i \bar{\Gamma}_i) + \bar{B}(\Theta_j \Delta_j \Pi_j) \big]^T + \beta (Y_j + \Theta_j \Delta_j \Pi_j X)^T R (K_j + \Theta_j \Delta_j \Pi_j) X \Big\} \prec 0$$

By applying the Schur complement and lemma 2, the latter inequality can be eventually written as.

$$\sum_{i=1}^{4}\sum_{j=1}^{4} \alpha_i(t) \alpha_j(t) \left\{ \begin{bmatrix} \Omega & Y_j^T & X & \sqrt{\beta} D \\ * & -\beta R^{-1} & 0 & 0 \\ * & * & -\beta Q^{-1} & 0 \\ * & * & * & -\lambda I \end{bmatrix} + \gamma_1 \begin{bmatrix} \bar{\Phi}_i \\ 0 \\ 0 \\ 0 \end{bmatrix} \begin{bmatrix} \bar{\Phi}_i \\ 0 \\ 0 \\ 0 \end{bmatrix}^T + \gamma_2 \begin{bmatrix} \bar{B}\Theta_j \\ \Theta_j \\ 0 \\ 0 \end{bmatrix} \begin{bmatrix} \bar{B}\Theta_j \\ \Theta_j \\ 0 \\ 0 \end{bmatrix}^T + \gamma_1^{-1} \begin{bmatrix} \bar{\Gamma}_i X \\ 0 \\ 0 \\ 0 \end{bmatrix} \begin{bmatrix} \bar{\Gamma}_i X \\ 0 \\ 0 \\ 0 \end{bmatrix}^T + \gamma_2^{-1} \begin{bmatrix} \bar{B}\Pi_j X \\ \Pi_j X \\ 0 \\ 0 \end{bmatrix} \begin{bmatrix} \bar{B}\Pi_j X \\ \Pi_j X \\ 0 \\ 0 \end{bmatrix}^T \right\} \prec 0$$

Where $\Omega = \bar{A}_i^T X + X \bar{A}_i + \bar{B} Y_j + Y_j^T \bar{B}^T$

Applying the Schur complement again, it is worth noticing that the above matrix inequality is equivalent to matrix inequality (27). That is

$$\sum_{i=1}^{4}\sum_{j=1}^{4} \alpha_i(t) \alpha_j(t) \Upsilon_{ii} \prec 0,$$

Therefore, the results of Theorem 1 are obtained from proposition 1 and proposition 2.

Next, we analyze the upper bound of the performance level as specified in equation (15). Considering Theorem 1, the (LMIs) (22)-(26) are solvable, which means that a set of convex solutions $(X, Y_j, H_i, \lambda, \beta, S, \gamma_1, \gamma_2, \gamma_3)$ is thus defined. These (LMIs) can be solved using several types of convex optimization algorithms, such as the SDPT3 solver. Furthermore, to achieve the optimal guaranteed cost control with a minimum bound on the performance level, the following optimization problem is proposed.

$$\min_{X, Y_j, H_i, \rho, S, N, \beta} \beta + tr(S) \tag{30}$$

Subject to (LMIs) (22)-(26)

$$\begin{bmatrix} S & \lambda T^T \\ \lambda T & \lambda I \end{bmatrix} \geq 0$$

If the given optimization problem has a feasible solution $(X, Y_j, H_i, \lambda, \beta, S, \gamma_1, \gamma_2, \gamma_3)$, then, the fuzzy control law $U(t)$ is an optimal non-fragile guaranteed cost tracking controller of the uncertain system (13) guaranteeing a minimum upper bound on the performance level $\bar{J}_{ot}$, with the control input bounded along each axis, where $\int_{t_0}^{t_f} Y_{tr}(\tau) Y_{tr}^T(\tau)\, d\tau = TT^T$.

Referring to [40], the minimization of the performance level $\beta + tr(S)$ leads to the minimization of the performance level (15). Consequently, by solving the minimization problem (30) a minimum value of the performance level is definitely obtained. The proof can be found in [40].

- Remark 1: From Theorem 1, it is worth noting that the gain matrices K_j are derived directly by setting one common positive definite matrix to address different objectives. However, this approach tends to be conservative in its solutions. To obtain an optimal solution and reduce this conservatism, it is necessary to explore the distinct parameter-dependent Lyapunov functions approach. This approach has the potential to make the problem less conservative.
- Remark 2: The proposed optimization problem focuses on enhancing the robust performance of orbit transfer by accounting for uncertainties and gain perturbations. The overall robustness of this approach will be improved for the orbit transfer process and has the potential to be extended to H_∞ control while considering uncertainties, where the optimization problem would involve minimizing the overall disturbance level of the controlled system. Investigating orbit transfer control with H_∞ and H_2 performance is a promising direction for future research.

4. Presentation of Results

In the simulation results section, four (LTI) models were developed for each operating point with the degree of satisfaction determined by equation (4). The membership functions are illustrated in Fig. 2 The four rule T-S fuzzy model as expressed in equation (3) is used to represent the nonlinear dynamics of spacecraft motion. The matrices A_i, $(i = 1, \ldots, 4)$ of the four subsystems are determined as

$$A_1 = \begin{bmatrix} 0 & 0 & 1 & 0 \\ 0 & 0 & 0 & \frac{1}{r_l} \\ -\frac{\mu}{r_h^3} & 0 & 0 & \frac{v_{\theta_s}}{r_l} \\ 0 & 0 & \frac{-v_{\theta_b}}{r_h} & 0 \end{bmatrix}, A_2 = \begin{bmatrix} 0 & 0 & 1 & 0 \\ 0 & 0 & 0 & \frac{1}{r_l} \\ -\frac{\mu}{r_l^3} & 0 & 0 & \frac{v_{\theta_b}}{r_l} \\ 0 & 0 & \frac{-v_{\theta_b}}{r_l} & 0 \end{bmatrix}, A_3 = \begin{bmatrix} 0 & 0 & 1 & 0 \\ 0 & 0 & 0 & \frac{1}{r_h} \\ -\frac{\mu}{r_h^3} & 0 & 0 & \frac{v_{\theta_s}}{r_h} \\ 0 & 0 & \frac{-v_{\theta_s}}{r_h} & 0 \end{bmatrix}, A_4 = \begin{bmatrix} 0 & 0 & 1 & 0 \\ 0 & 0 & 0 & \frac{1}{r_h} \\ -\frac{\mu}{r_h^3} & 0 & 0 & \frac{v_{\theta_b}}{r_h} \\ 0 & 0 & \frac{-v_{\theta_b}}{r_h} & 0 \end{bmatrix}$$

According to the nonlinear system described in (2), only A contains nonlinear parameters. Since the matrix A has two nonlinear parameters, four plant rules are assigned, with the fuzzy variables falling within the following ranges:

$$r \in [r_l \quad r_h], v_\theta \in [v_{\theta_s} \quad v_{\theta_b}].$$

Here, the range of r and v_θ are given as $6878 \leq r \leq 42164$ (Km) and $3.0746 \leq v_\theta \leq 7.612$ (Km/s). The control input $U(t)$ is subjected to

$$-10^2 \leq U_\kappa \leq 10^2, \quad \kappa = (r, \theta)$$

The orbit transfer is analyzed by considering two different maneuvers: Starting with the first case (Case I), this case focuses on identifying the minimum performance level under nominal conditions. In the second case (Case II), the aim is to determine the minimum performance level for an orbit transfer while accounting for uncertainties and gain perturbations. The objective of this case is to demonstrate the robustness of our system. Additionally, a comparison with an existing

control method has been performed to validate our model. The weighting matrices Q and R are respectively selected as $1 \times 10^{+3} I_{4\times4}$ and $1 \times 10^{+4} I_{2\times2}$ for both cases. The diagonal elements of Q are chosen largely because the state variables are crucial in the system dynamics. The diagonal elements of R are also used to penalize the control input. Higher values are selected in order to reduce the magnitude of the control inputs.

4.1. Case I: Orbit Transfer with Nominal Conditions

In this case, we assume that the spacecraft performs a transfer from its initial orbit with radial position $r = 24505.9\ (Km)$ and transverse position $\theta = \frac{3\pi}{2}\ (Rad)$. Thus, the initial state vector can be written as $W_I(0) = [24505.9, \frac{3\pi}{2}, 0, 4.03304, 0, 0]^T$. Then, we assume that the tracking position located on the final orbit is defined as $Ytr_I = \left[42165, \frac{\pi}{2}\right]^T$. By solving the optimization problem (30) using the state and output vectors of this case, one obtains the upper bound of the cost $\bar{J}_{otI} = 2.714 \times 10^{+3}$. Consequently, the resulting gain feedback matrices $K_{i_{caseI}}$ are expressed as follows

$$K_{1_{caseI}} = \begin{bmatrix} 3.1169\times10^{-3} & 2.6441\times10^{-3} & 6.2103\times10^{-2} & 3.3655\times10^{-4} & -7.1476\times10^{-5} & 6.2267\times10^{-6} \\ 2.9875\times10^{-4} & 5.5827\times10^{-1} & 1.4257\times10^{-2} & 1.0403\times10^{-2} & 9.5481\times10^{-6} & 1.1921\times10^{-3} \end{bmatrix}$$

$$K_{2_{caseI}} = \begin{bmatrix} -2.9187\times10^{-3} & 2.4287\times10^{-3} & -5.8496\times10^{-2} & -8.2538\times10^{-4} & -6.6895\times10^{-5} & 3.2871\times10^{-6} \\ -1.5552\times10^{-4} & -5.3420\times10^{-1} & -0.4916\times10^{-1} & -1.0433\times10^{-1} & -3.7362\times10^{-5} & -1.1319\times10^{-3} \end{bmatrix}$$

$$K_{3_{caseI}} = \begin{bmatrix} -3.1423\times10^{-3} & 2.0997\times10^{-4} & -6.2401\times10^{-2} & -4.8788\times10^{-5} & -7.1786\times10^{-5} & 4.6064\times10^{-6} \\ 9.9185\times10^{-4} & -4.2626\times10^{-1} & -3.4702\times10^{-2} & -8.8672\times10^{-3} & 3.2690\times10^{-5} & -7.1360\times10^{-4} \end{bmatrix}$$

$$K_{4_{caseI}} = \begin{bmatrix} -3.1433\times10^{-3} & 2.1013\times10^{-3} & -6.2461\times10^{-2} & -1.1962\times10^{-4} & -7.1920\times10^{-5} & 5.1959\times10^{-6} \\ 7.4693\times10^{-4} & -4.2643\times10^{-1} & -8.1453\times10^{-3} & -8.8811\times10^{-3} & 2.6453\times10^{-5} & -7.1390\times10^{-4} \end{bmatrix}$$

Then, tracking performance results associated are listed in the following Fig. 3 and Fig. 4.

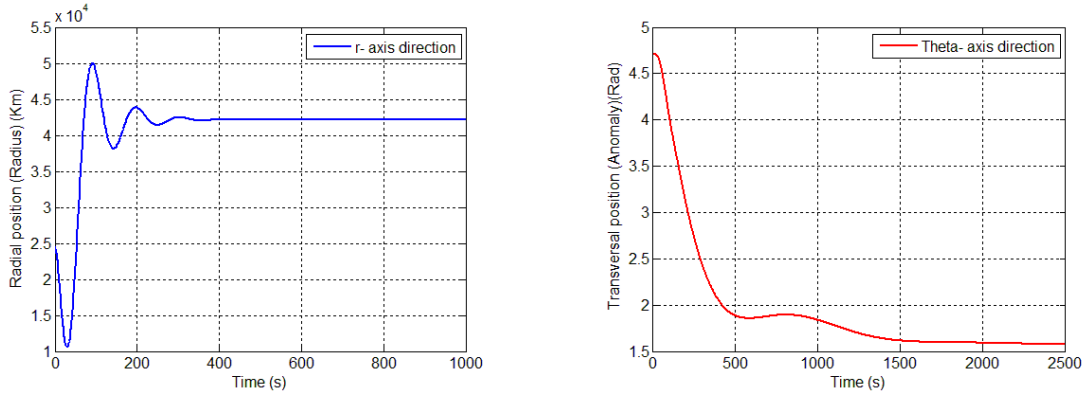

Fig. 3. Positional outputs for orbit transfer in nominal conditions

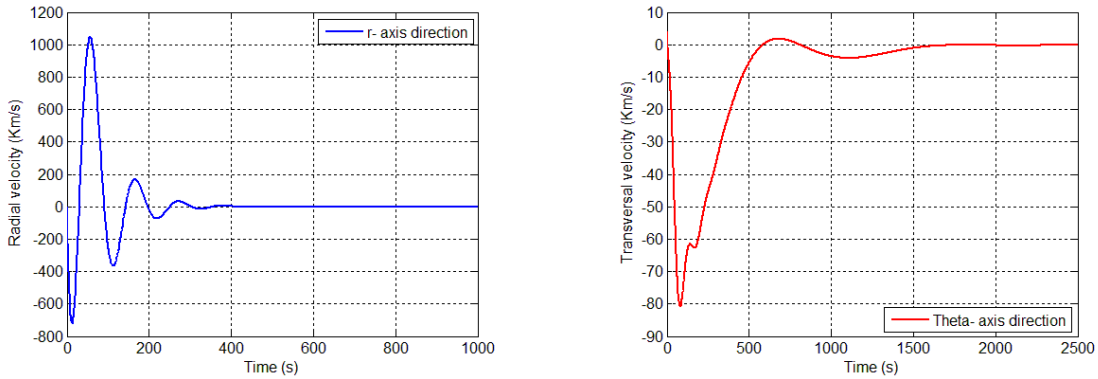

Fig. 4. Velocity change for orbit transfer in nominal conditions

Fig. 3 illustrates the positional output of spacecraft characterized by radius $r$and anomalyθ. Fig. 4 depicts the velocity change of the spacecraft during the obit transfer process. It should be noticed that when the positional outputs of the system converge to the tracking outputs, the radial and transverse velocities instantly approach zero, signifying that the spacecraft has reached and maintained its tracking position.

With the control law (12), the spacecraft starts the orbit transfer from its initial position $(r_0, \theta_0) = (24505.9, 4.712)$, with initial velocity $\left(\upsilon_{r_0}, \upsilon_{\theta_0}\right) = (0, 4.03304)$as depicted in Fig. 3 and Fig. 4. It can be seen from Fig. 3 that the positional output of the spacecraft converges asymptotically to the tracking position (r_{tr}, θ_{tr}) at different points in time. Specifically, the radius converges to its reference in a time span of $400\ s$, while the anomaly converges to its reference over a period of $1600s$. The radial position changes more rapidly than the angular position during an orbit transfer due to several factors, including the interaction between orbital velocity, conservation of angular momentum, and the shape of the orbit (which is often elliptical). The spacecraft's velocity is not uniform throughout the orbit, but varies based on its distance from the central body, resulting in more rapid changes in radial position relative to angular position. This can be explained by the fact that the spacecraft covers a larger distance per unit time in the radial direction compared to the angular direction due to its higher velocity.

Fig. 5, illustrates the positional tracking errors of the spacecraft during its maneuver. These tracking results are obtained by incorporating the output tracking error$lim\, e\,(t) = \lim_{t\to\infty}(Y(t) - Y_{tr}(t)) = 0$ into the designed controller. It is important to emphasize that the spacecraft reaches its final orbit by reducing the radial trackinFigg error to zero$\lim_{t\to\infty}(r(t) - r_{tr}(t)) = 0$. Then, the phase difference between the transverse position and the desired position decreases as the transverse tracking error approaches zero $\lim_{t\to\infty}(\theta(t) - \theta_{tr}(t)) = 0$. When both errors reach zero, it indicates that the spacecraft has accurately reached the desired tracking position.

The required input accelerations during the orbit transfer maneuver along each direction are depicted in Fig. 6. The maximum required values of thrust along r - and θ -axis are $61.3\ (N/kg)$ and $41.3 \times 10^{-2}\ (N/kg)$ respectively, it is worth noting that both of thrust values are below the thrust upper bound. It can be concluded that the input constraint works correctly with the designed controller.

Simulations were conducted to compare the (FNGCC) with the (OFNGCC) to show the better performance achieved. Using the nominal system with input constraints, the performance level of the (FNGCC) is determined by applying Theorem 1, while the optimal solution for the (OFNGCC) controller is obtained by solving the optimization problem in (30). The results for different upper-bound values are listed in Table 1.

Table 1. Upper bound values of the performance level

Controller	$\bar{J}_{ot}$
FNGCC	$2.9825 \times 10^{+3}$
OFNGCC	$2.7140 \times 10^{+3}$

According to Table 1, the OFNGCC shows a more satisfactory performance level than the FNGCC, indicating that optimal guaranteed cost control has been achieved with the OFNGCC.

On the other hand, analyses have been conducted to illustrate the effect of the input constraint on system performance. The results for different upper bound values on the nominal system are presented in Table 2.

From Table 2, the analysis demonstrates how input constraints increase the upper bound of the performance level of the system. The performance level will likely be lower because the controller can apply optimal control without restrictions.

Table 2. Upper bound values of the performance level on nominal system

Nominal system	$\bar{J}_{ot}$
System Without IC	$1.422 \times 10^{+3}$
System With IC	$2.714 \times 10^{+3}$

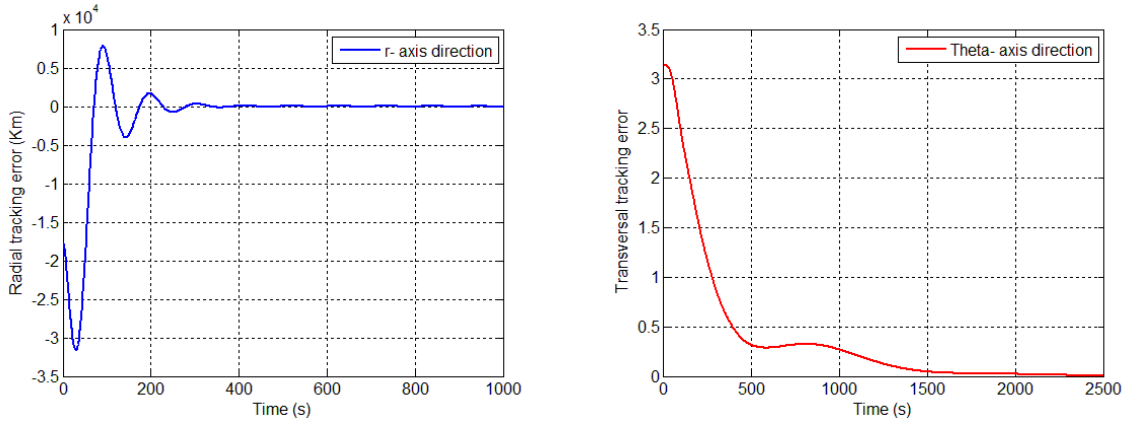

Fig. 5. Positional tracking errors for orbit transfer in nominal conditions

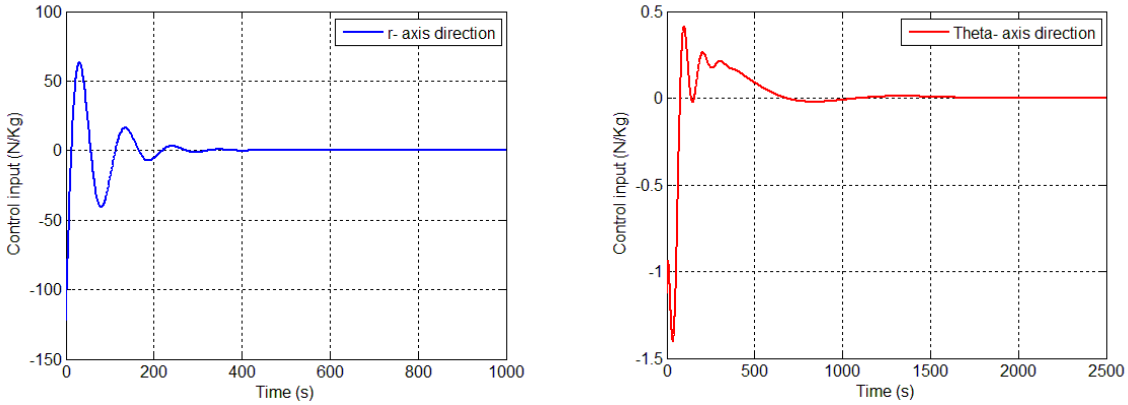

Fig. 6. Input acceleration for orbit transfer in nominal conditions

4.2. Case II: Orbit Transfer with Uncertainty

Assuming that the spacecraft moves from the initial low Earth circular orbit of radius $r = 6878(km)$, and transverse position $\theta = \pi\,(rad)$. Thus, the initial state vector can be expressed as$W_{II}(0) = [\,6878,\pi,0,7.612,0,0\,]^{T}$. Then, we presume that the reference position is located on the final orbit and defined as$Ytr_{II} = [24505.9,0]^{T}$.

According to the structure of the system matrices, the uncertainty matrices that describe the parameter errors of the system are of the form

$$\Phi_i = \sigma \times \begin{bmatrix} 1 & 0 & 0 & 1 \\ 0 & 1 & 0 & 1 \\ 1 & 1 & 0 & 0 \\ 1 & 0 & 1 & 1 \end{bmatrix}, \Gamma_i = \delta \times \begin{bmatrix} 1 & 0 & 0 & 1 \\ 0 & 1 & 1 & 0 \\ 0 & 1 & 0 & 1 \\ 1 & 0 & 1 & 1 \end{bmatrix},$$

Moreover, the uncertainty matrices representing the gain perturbations have the following form

$$\Phi_i = \rho \times \begin{bmatrix} 1 & 1 & 0 & 0 & 0 & 0 \\ 1 & 0 & 1 & 0 & 0 & 0 \end{bmatrix}, \Pi_i = \tau \times \begin{bmatrix} 1 & 0 \\ 1 & 0 \end{bmatrix}.$$

Whereσ,δ,ρ and τ represent magnitudes of uncertainty by which we can add, remove or change the values of uncertainty parameters. We consider the following values

$$\sigma = 1 \times 10^{-3}, \delta = 1 \times 10^{-2}, \rho = 1 \times 10^{-2} \text{ and } \tau = 1 \times 10^{-3}$$

The uncertainty matricesΦ_i,Γ_i, Θ_i and Π_i are assumed to be equal for the four rules of the system. Solutions to the optimization problem (30) give the minimum performance level$\bar{J}_{ot} = 5.146 * 10^{+3}$. Then, the resulting gain matrices $K_{i_{caseII}}$ are listed as follows

$$K_{1_{caseII}} = \begin{bmatrix} -0.013416 & -0.044499 & -0.1195 & -0.0007686 & -0.0006772 & -0.00013302 \\ -0.003351 & -1.4067 & -0.025648 & -0.016105 & -0.00019825 & -0.0037992 \end{bmatrix}$$

$$K_{2_{caseII}} = \begin{bmatrix} -0.013372 & -0.048787 & -0.11902 & -0.0013695 & -0.00067465 & -0.00014664 \\ -0.0031795 & -1.4043 & -0.023911 & -0.016147 & -0.00019073 & -0.0037917 \end{bmatrix}$$

$$K_{3_{caseII}} = \begin{bmatrix} -0.013432 & -0.019278 & -0.11968 & -0.00019756 & -0.00067804 & -5.4997e\text{-}05 \\ -0.0045009 & -1.2374 & -0.037173 & -0.013836 & -0.00025345 & -0.0030201 \end{bmatrix}$$

$$K_{4_{caseII}} = \begin{bmatrix} -0.01343 & -0.017359 & -0.11966 & -0.00028145 & -0.00067794 & -4.9058e\text{-}05 \\ -0.0044837 & -1.2371 & -0.036995 & -0.013845 & -0.00025283 & -0.0030193 \end{bmatrix}$$

Alternatively, according to [40], a conventional guaranteed cost memoryless state-feedback controller K_j^*can also be obtained by the proposed model along with the minimum performance level$\bar{J}^* = 4.705 * 10^{+3}$. However, compared to the method proposed in [40], the minimum performance level obtained through this paper is higher, due to the consideration of input constraints. Therefore, the resulting gain matrices $K_i^*$are listed as follows.

$$K_1^* = \begin{bmatrix} -0.023251 & -0.0087141 & -0.16163 & -0.00086421 & -0.0014812 & -5.0134\times10^{-5} \\ -5.5223\times10^{-7} & -0.81999 & -0.0033983 & -0.020739 & -2.6516\times10^{-5} & -0.0034184 \end{bmatrix}$$

$$K_2^* = \begin{bmatrix} -0.023243 & -0.0041781 & -0.16158 & -0.0013507 & -0.001481 & -3.014 \times 10^{-5} \\ -0.00030937 & -0.82006 & -0.0053271 & -0.020746 & -4.9293 \times 10^{-5} & -0.0034183 \end{bmatrix}$$

$$K_3^* = \begin{bmatrix} -0.023252 & -0.017459 & -0.16163 & -0.00060163 & -0.001481 & -9.4245 \times 10^{-5} \\ 0.00017788 & -0.41936 & -0.0025366 & -0.019484 & -9.214 \times 10^{-6} & -0.0013875 \end{bmatrix}$$

$$K_4^* = \begin{bmatrix} -0.023252 & -0.016425 & -0.16163 & -0.00067914 & -0.0014811 & -8.9235 \times 10^{-5} \\ 0.00012501 & -0.41942 & -0.002869 & -0.019485 & -1.3101 \times 10^{-5} & -0.0013878 \end{bmatrix}$$

Then, the tracking performance results for both control methods are presented in Fig. 7 and Fig. 8.

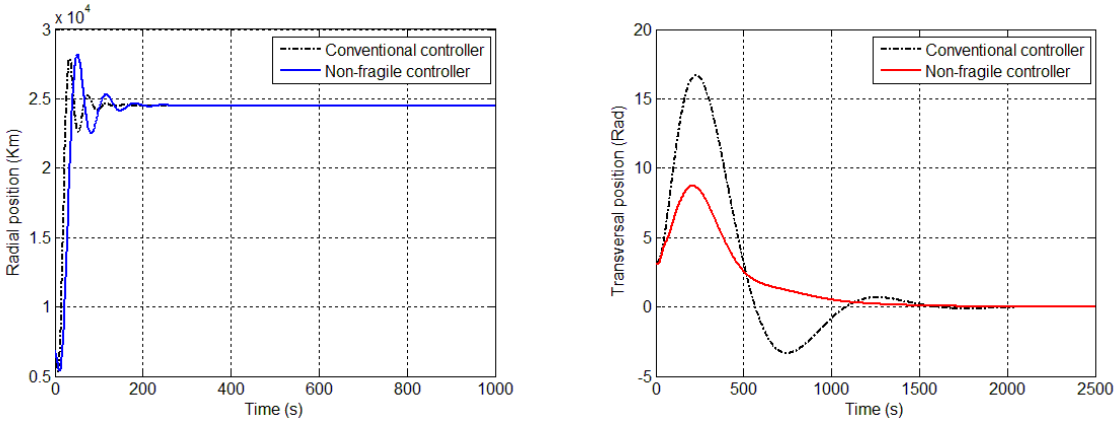

Fig. 7. Positional outputs of orbit transfer

Fig. 7, Fig. 8 provide a comparison between the results using the model developed in this research and the results using the method in [40]. Notably, these figures demonstrate that both methods can effectively meet the tracking requirements for position and velocity, which prove the validity of our model. Furthermore, for our model, the results demonstrate the robustness of the proposed model against model and controller uncertainties. It is also noted that the impact of the uncertainties on the system is more noticeable in the transverse direction than in the radial

direction. This can be explained by the fact that in polar coordinates, the angular component often requires more precise control because it governs the spacecraft's ability to maintain its orientation and trajectory. Uncertainties in the transverse direction can therefore have larger cascading effects than similar uncertainties in the radial direction.

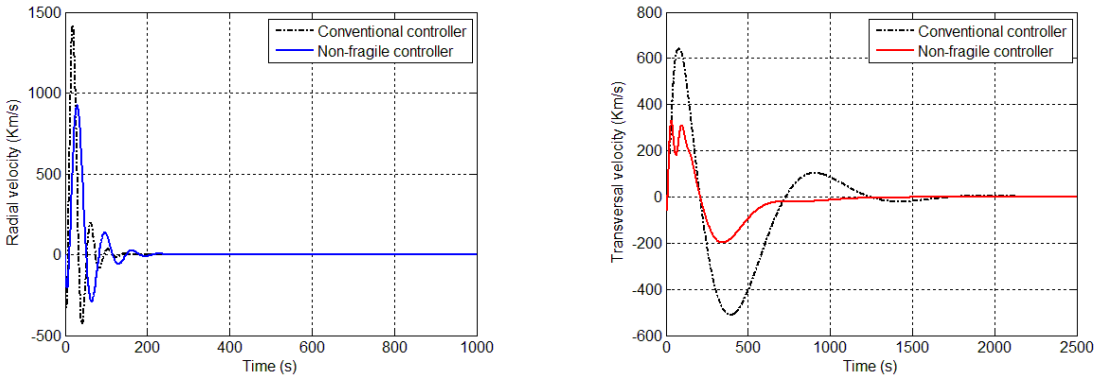

Fig. 8. Velocity change of orbit transfer

Considering the uncertainty parameters, it's important to note that varying the parameter errors can lead to different results. If these parameters exceed certain values, the system may become unstable, rendering the problem unsolvable. Three scenarios have been considered to determine the permitted ranges of the uncertainty values:

- Scenario 1: considering uncertainties in the model and controller, and setting all magnitudes equal (i.e., $\sigma = \delta = \rho = \tau$). The permitted range of all magnitudes is$[0, \quad 0.01]$. However, in the case where ($\sigma \neq \delta \neq \rho \neq \tau$), the range of a parameter can be determined by changing that parameter and keeping the others constants.
- Scenario 2: considering only model uncertainties ($\rho = \tau = 0$) with($\sigma = \delta$), the permitted range of σ and δ is$[0, \quad 0.0125]$.
- Scenario 3: considering only controller uncertainties ($\sigma = \delta = 0$) with($\rho = \tau$), the permitted range of $\rho$and τ is$[0, \quad 0.011]$. Alternatively, by considering the cases where ($\sigma \neq \delta$) and($\rho \neq \tau$), the range of one parameter can be determined by changing a parameter and holding the other constant for each scenario.

Fig. 9 illustrates the input thrust required by our controller in comparison to the conventional controller. Despite the presence of uncertainties in the controller, the non-fragile controller requires less thrust due to the use of input constraints. Nevertheless, both systems maintain stability and provide good tracking performance, even in the presence of uncertainties. This demonstrates that the spacecraft control system is sufficiently robust to handle these uncertainties effectively.

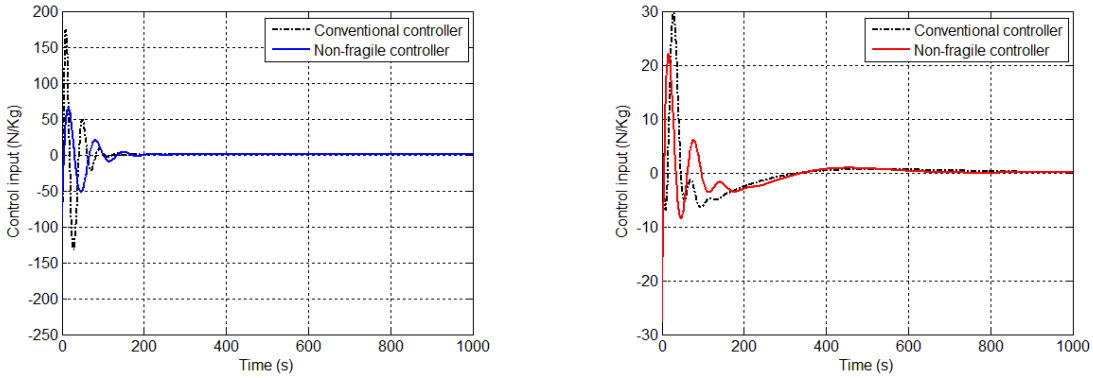

a. Radiale direction b. Transversal direction

Fig. 9. Input acceleration of orbit transfer

Furthermore, It is important to highlight that the feasibility of the (LMIs) outlined in Theorem 1 depends on the upper bound of thrust. Specifically, small values of $U_r$and U_θ might cause infeasibility of (LMIs) and the input constraint may not function correctly. As a result, it is imperative that the upper bound values for thrust along both axes remain greater than 25 *(N/Kg)*. Another feasibility constraint is that the initial and final state values of the spacecraft must fall within the specified ranges chosen for this study. If the values are outside these ranges, the model may not function correctly. Therefore, it is necessary to adjust the ranges for other orbital transfer missions with initial or final state falls beyond these limits.

Finally, to illustrate the complete orbit transfer, Fig. 10 depicts an overview of the whole orbit transfer trajectory. It is clear that the spacecraft is asymptotically transferred to the final orbit and reaches the designated tracking position. From the results obtained, it can be concluded that the fuzzy tracking control methodology offers satisfactory performance for the orbit transfer with the newly constructed model under limited thrust and minimum performance level, irrespective of whether the system is subjected to uncertainty and gain perturbations.

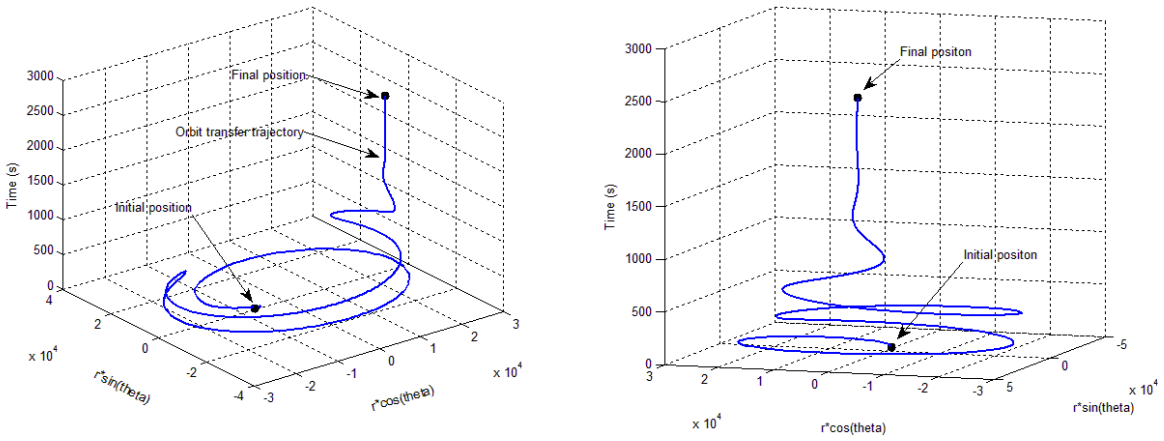

a. Side view 1 b. Side view 2

Fig. 10. Overview of orbit transfer trajectory

5. Conclusion

This paper has presented a fuzzy gain-scheduling guaranteed cost tracking control for spacecraft orbit transfer maneuver in a circular orbit, subject to parameter uncertainty, gain perturbations, and input constraint. The dynamics of spacecraft is described by polar coordinates. A (T-S) fuzzy approach based on the gain scheduling technique is used to linearize the spacecraft dynamics. A tracking design was implemented to enable the spacecraft to follow the reference position and achieve the final orbit. By applying Lyapunov theory, the orbit transfer problem is converted into a convex optimization problem with (LMI) constraints. With the designed controller, the orbit transfer process is successfully achieved with minimum thrust and performance level under a specified bound. The numerical examples have been conducted with four (LTI) models covering the entire operating range of the system. As the number of (LTI) models is increased, the fuzzy model more accurately represents the characteristics of the original system. However, this also makes it more challenging to find a solution that satisfies the (LMIs) in Theorem 1. Furthermore, this model is developed for planar orbit transfer maneuvers in a circular orbit, with the advantage of enabling any long-distance maneuver from the known initial orbit to the final orbit. Moreover, this model can also be applied to more complex missions, such as formation flying, or orbital rendezvous between two active spacecraft. It would be advantageous to implement a simultaneous stabilization control strategy, enabling the stabilization of multiple spacecraft within the formation or the orbital rendezvous.

Author Contribution: All authors contributed equally to the main contributor to this paper. All authors read and approved the final paper.

Funding: This research received no external funding from any company.

Conflicts of Interest: The authors declare no conflicts of interest that are relevant to the content of this article.

References

[1] S. Hernandez and M. R. Akella, "Lyapunov-based guidance for orbit transfers and rendezvous in levi-civita coordinates," *Journal of Guidance, Control, and Dynamics*, vol. 37, no. 4, pp. 1170-1181, 2014, https://doi.org/10.2514/1.62305.

[2] D. Sanna, E. M. Leonardi, G. De Angelis, and M. Pontani, "Optimal Impulsive Orbit Transfers from Gateway to Low Lunar Orbit," *Aerospace*, vol. 11, no. 6, p. 460, 2024, https://doi.org/10.3390/aerospace11060460.

[3] X. Wang, Z. Wang, and Y. Zhang, "Automated orbital transfer and hovering control using artificial potential," *Mathematical Problems in Engineering*, vol. 2019, no. 1, pp. 1-16, 2019, https://doi.org/10.1155/2019/6186283.

[4] H. Li, H. Baoyin and F. Topputo, "Neural Networks in Time-Optimal Low-Thrust Interplanetary Transfers," *IEEE Access*, vol. 7, pp. 156413-156419, 2019, https://doi.org/10.1109/ACCESS.2019.2946657.

[5] Y. Wang, C. Han, and X. Sun, "Optimization of low-thrust Earth-orbit transfers using the vectorial orbital elements," *Aerospace Science and Technology*, vol. 112, p. 106614, 2021, https://doi.org/10.1016/j.ast.2021.106614.

[6] Z. Wang and M. J. Grant, "Optimization of minimum-time low-thrust transfers using convex programming," *Journal of Spacecraft and Rockets*, vol. 55, pp. 586-598, 2018, https://doi.org/10.2514/1.A33995.

[7] W. Clohessy and R. Wiltshire, "Terminal guidance system for satellite rendezvous," *Journal of the aerospace sciences*, vol. 27, no. 9, pp. 653-658, 1960, https://doi.org/10.2514/8.8704.

[8] T. Takagi and M. Sugeno, "Fuzzy identification of systems and its applications to modeling and control," *Readings in Fuzzy Sets for Intelligent Systems*, pp. 387-403, 1985, https://doi.org/10.1016/B978-1-4832-1450-4.50045-6.

[9] C. Fantuzzi and R. Rovatti, "On the approximation capabilities of the homogeneous Takagi-Sugeno model," *Proceedings of IEEE 5th International Fuzzy Systems*, vol. 2, pp. 1067-1072, 1996, https://doi.org/10.1109/FUZZY.1996.552326.

[10] Hao Ying, "General SISO Takagi-Sugeno fuzzy systems with linear rule consequent are universal approximators," *IEEE Transactions on Fuzzy Systems*, vol. 6, no. 4, pp. 582-587, 1998, https://doi.org/10.1109/91.728456.

[11] K. Tanaka and H. O. Wang, "Fuzzy control systems design and analysis: a linear matrix inequality approach," *John Wiley & Sons*, 2004, https://doi.org/10.1002/0471224596.

[12] A. Benzaouia and A. E. Hajjaji, "Advanced Takagi-Sugeno Fuzzy Systems," *Springer*, 2016, https://doi.org/10.1007/978-3-319-05639-5.

[13] X. Su, C. P. Chen, and Z. Liu, "Adaptive fuzzy control for uncertain nonlinear systems subject to full state constraints and actuator faults," *Information Sciences*, vol. 581, pp. 553-566, 2021, https://doi.org/10.1016/j.ins.2021.09.055.

[14] S. Ahmad, S. Ali, and R. Tabasha, "The design and implementation of a fuzzy gain-scheduled PID controller for the Festo MPS PA compact workstation liquid level control," *Engineering Science and Technology, an International Journal*, vol. 23, no. 2, pp. 307-315, 2020, https://doi.org/10.1016/j.jestch.2019.05.014.

[15] M. Aghaseyedabdollah, M. Abedi, and M. Pourgholi, "Interval type-2 fuzzy sliding mode control for a cable-driven parallel robot with elastic cables using metaheuristic optimization methods," *Mathematics*

and Computers in Simulation, vol. 218, pp. 435-461, 2024, https://doi.org/10.1016/j.matcom.2023.11.036.

[16] Z. Du, Y. Kao, J. H. Park, X. Zhao, and J. Sun, "Fuzzy event-triggered control for nonlinear networked control systems," *Journal of the Franklin Institute*, vol. 359, no. 6, pp. 2593-2607, 2022, https://doi.org/10.1016/j.jfranklin.2022.02.027.

[17] K. H. Nguyen and S. H. Kim, "Improved sampled-data control design of TS fuzzy systems against mismatched fuzzy-basis functions," *Applied Mathematics and Computation*, vol. 428, p. 127150, 2022, https://doi.org/10.1016/j.amc.2022.127150.

[18] C. Hoffmann and H. Werner, "A Survey of Linear Parameter-Varying Control Applications Validated by Experiments or High-Fidelity Simulations," *IEEE Transactions on Control Systems Technology*, vol. 23, no. 2, pp. 416-433, 2015, https://doi.org/10.1109/TCST.2014.2327584.

[19] J. S. Shamma and M. Athans, "Guaranteed properties of gain scheduled control for linear parameter-varying plants," *Automatica*, vol. 27, no. 3, pp. 559-564, 1991, https://doi.org/10.1016/0005-1098(91)90116-J.

[20] Z. Zhang, Y. Shi, and H. Han, "Multivariate Attention-Based Orbit Uncertainty Propagation and Orbit Determination Method for Earth–Jupiter Transfer," *Applied Sciences*, vol. 14, no. 10, p. 4263, 2024, https://doi.org/10.3390/app14104263.

[21] M. S. Mohammadi and A. Naghash, "Robust optimization of impulsive orbit transfers under actuation uncertainties," *Aerospace Science and Technology*, vol. 85, pp. 246-258, 2019, https://doi.org/10.1016/j.ast.2018.11.026.

[22] P. Kuchynka, M. M. Serrano, K. Merz, and J. Siminski, "Uncertainties in GPS-based operational orbit determination: A case study of the Sentinel-1 and Sentinel-2 satellites," *The Aeronautical Journal*, vol. 124, no. 1276, pp. 888-901, 2020, https://doi.org/10.1017/aer.2020.8.

[23] Y.- Song, J. Bae, Y. Kim, and B. Kim, "Uncertainty requirement analysis for the orbit, attitude, and burn performance of the 1st lunar orbit insertion maneuver," *Journal of Astronomy and Space Sciences*, vol. 33, no. 4, pp. 323-333, 2016, https://doi.org/10.5140/JASS.2016.33.4.323.

[24] Y. Yang and Y. He, "Non-fragile observer-based robust control for uncertain systems via aperiodically intermittent control," *Information Sciences*, vol. 573, pp. 239-261, 2021, https://doi.org/10.1016/j.ins.2021.05.046.

[25] A. Hakimzadeh and V. Ghaffari, "Designing of non-fragile robust model predictive control for constrained uncertain systems and its application in process control," *Journal of Process Control*, vol. 95, pp. 86-97, 2020, https://doi.org/10.1016/j.jprocont.2020.10.004.

[26] J. Zhao *et al*., "Non-fragile robust output feedback control of uncertain active suspension systems with stochastic network-induced delay," *Nonlinear Dynamics*, vol. 111, pp. 8275-8291, 2023, https://doi.org/10.1007/s11071-023-08267-3.

[27] J. Wang, H. Li, and X. Zhang, "Non-fragile guaranteed cost control of nonlinear switched systems with actuator saturation," *Transactions of the Institute of Measurement and Control*, vol. 45, no. 13, pp. 2602-2610, 2023, https://doi.org/10.1177/01423312231152931.

[28] X. Yang, H. Gao, "Guaranteed Cost Output Tracking Control for Autonomous Homing Phase of Spacecraft Rendezvous," *Journal of Aerospace Engineering*, vol. 24, no. 4, pp. 478-487, 2011, https://doi.org/10.1061/(ASCE)AS.1943-5525.0000085.

[29] D. Sheng, X. Yang, and H. R. Karimi, "Robust control for autonomous spacecraft evacuation with model uncertainty and upper bound of performance with constraints," *Mathematical Problems in Engineering*, vol. 2014, no. 1, pp. 1-16, 2014, https://doi.org/10.1155/2014/589381.

[30] X. Yang, H. Gao, and P. Shi, "Robust orbital transfer for low earth orbit spacecraft with small-thrust," *Journal of the Franklin Institute*, vol. 347, no. 10, pp. 1863-1887, 2010, https://doi.org/10.1016/j.jfranklin.2010.10.006.

[31] X. Gao, K. L. Teo, and G. Duan, "Non-fragile guaranteed cost control for robust spacecraft orbit transfer with small thrust," *IMA Journal of Mathematical Control and Information*, vol. 28, no. 4, pp. 507-524, 2011, https://doi.org/10.1093/imamci/dnr024.

[32] G. Xiangyu, Z. Xian, T. Julong, and L. Jiaojiao, "No-fragile H∞ guaranteed cost control design for spacecraft rendezvous," *IFAC-PapersOnLine*, vol. 48, no. 28, pp. 1331-1336, 2015, https://doi.org/10.1016/j.ifacol.2015.12.316.

[33] X. Gao, K. L. Teo, and G. Duan, "Non-fragile robust H∞ control for uncertain spacecraft rendezvous system with pole and input constraints," *International Journal of Control*, vol. 85, no. 7, pp. 933-941, 2012, https://doi.org/10.1080/00207179.2012.669848.

[34] A. Zavoli and G. Colasurdo, "Indirect optimization of finite-thrust cooperative rendezvous," *Journal of Guidance, Control, and Dynamics*, vol. 38, no. 2, pp. 304-314, 2015, https://doi.org/10.2514/1.G000531.

[35] A. Fujimori and H. Tsunetom, Z. Wu, "Gain-scheduled control using fuzzy logic and its application to flight control," *Journal of guidance, control, and dynamics*, vol. 22, no. 1, pp. 175-178, 1999, https://doi.org/10.2514/2.7623.

[36] I. R. Petersen, "A stabilization algorithm for a class of uncertain linear systems," *Systems & control letters*, vol. 8, no. 4, pp. 351-357, 1987, https://doi.org/10.1016/0167-6911(87)90102-2.

[37] S. Boyd, L. E. Ghaoui, E. Feron, and V. Balakrishnan, "Linear matrix inequalities in system and control theory," *Studies in Applied and Numerical Mathematics*, 1994, https://doi.org/10.1137/1.9781611970777.

[38] H. D. Tuan, P. Apkarian, T. Narikiyo and Y. Yamamoto, "Parameterized linear matrix inequality techniques in fuzzy control system design," *IEEE Transactions on Fuzzy Systems*, vol. 9, no. 2, pp. 324-332, 2001, https://doi.org/10.1109/91.919253.

[39] D. Wang, J. Qiao and L. Cheng, "An Approximate Neuro-Optimal Solution of Discounted Guaranteed Cost Control Design," *IEEE Transactions on Cybernetics*, vol. 52, no. 1, pp. 77-86, 2022, https://doi.org/10.1109/TCYB.2020.2977318.

[40] L. Yu and J. Chu, "An LMI approach to guaranteed cost control of linear uncertain time-delay systems," *Automatica*, vol. 35, no. 6, pp. 1155-1159, 1999, https://doi.org/10.1016/S0005-1098(99)00007-2.